Cloud fraction and cloud top pressure retrieval
from GOME compared with ATSR-2 measurements

R.B.A. Koelemeijer and P. Stammes

Royal Netherlands Meteorological Institute (KNMI)
P.O. Box 201, 3730 AE De Bilt, The Netherlands

Abstract

Cloud fraction and cloud top pressure are the most important cloud parameters needed for accurate ozone column retrievals from the Global Ozone Monitoring Experiment (GOME). Presently, cloud top pressure is assumed a-priori in the ozone column retrieval. Here we report on an improved cloud scheme which can be used for ozone column retrieval, which simultaneously retrieves cloud fraction and cloud top pressure. This algorithm (FRESCO) makes use of radiances measured in three narrow wavelength intervals inside and outside the oxygen A-band, namely at 758 nm (no absorption), 761 nm (strong absorption), and 765 nm (moderate absorption).

The results are compared to cloud fractions and cloud top pressures derived from collocated ATSR-2 measurements. To this end, a cloud detection algorithm is used to separate clear and cloudy pixels in ATSR-2 images. The brightness temperatures of the cloudy pixels as measured by ATSR-2 are related to cloud top pressures using ECMWF profiles. Generally, the results from GOME and ATSR-2 agree well. The average difference in cloud fraction is 0.05, the RMS difference is 0.10. The average difference in cloud top pressure is 65 hPa, the root-mean-square (RMS) difference is 112 hPa.

1 Introduction

The Global Ozone Monitoring Experiment (GOME), launched on board the ERS-2 satellite of the European Space Agency, is a spectrometer measuring the Earth's reflectivity between 240 and 790 nm, with a spectral resolution of 0.2–0.4 nm (Burrows, et al., 1999). The ground pixel size of GOME can be varied between 40×80 km^2 and 40×320 km^2. The primary geophysical product of GOME is the ozone column. Since clouds are one of the largest potential error sources in ozone column retrievals, the presence of clouds should be taken into account in such retrievals. Therefore, as part of the operational GOME ozone column retrieval algorithm, cloud fraction is derived by the Initial Cloud Fitting Algorithm (ICFA) (Kuze and Chance, 1994; DRL, 1994), which makes use of the spectral reflectivity between 758 and 778 nm, which encloses the O$_2$ A-band. In ICFA, cloud top pressure is assumed a priori, and is taken from the International Satellite Cloud Climatology Project (ISCCP) database (Rossow and Garder, 1993). However, the actual cloud top pressure may be different from the climatological mean value. Moreover, errors in the ICFA cloud fraction may occur due to errors in the assumed cloud top pressure (Koelemeijer and Stammes, 1999a). The aim of this work is to improve the ozone column retrieval by deriving both cloud fraction and cloud top pressure from the oxygen A-band.

Retrieval of cloud pressure from the oxygen A-band has a long history beginning with the first suggestions by Yamamoto and Wark (1962) and Chapman (1962). The first satellite measurements were made rapidly afterwards, from Gemini-5 in August 1965 (Saiedy, 1967). Investigations on the theoretical side were made by e.g. Wu (1985) (impact of multiple scattering inside clouds to some extent), Fischer and Grassl (1991) (detailed sensitivity study cloud top pressure retrieval), and O'Brien
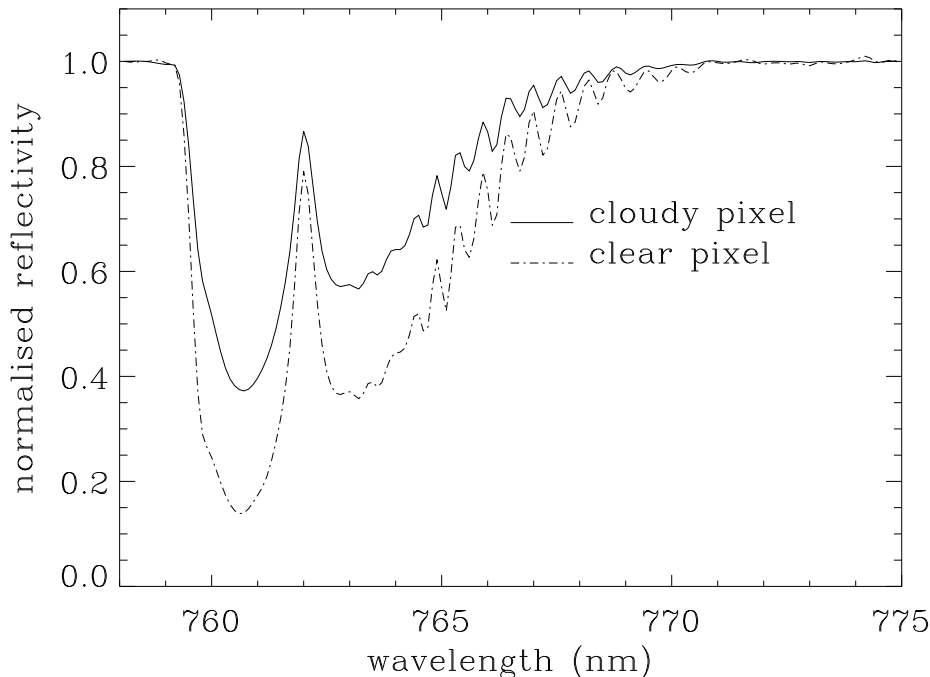
Figure 1: GOME measurements of the oxygen A-band. The spectra are normalized to unity at 758 nm. The solar zenith angle is 30° for the clear pixel and 21° for the cloudy pixel. The spectral resolution of GOME at these wavelengths is about 0.4 nm; the spectral sampling is about 0.2 nm.

and Mitchell (1992) (error estimates for surface pressure retrieval). With the launch of the GOME (Burrows, et al., 1999) and POLDER (Vanbauce et al., 1998) instruments in 1995 and 1996, respectively, the first routine space based measurements of the oxygen A-band have become available. The cloud fractions and cloud top pressures derived from GOME are not only useful for ozone column retrieval, but may also be useful for climate studies, as GOME provides these cloud parameters on the spatial scale of GCMs.

2   Cloud retrieval method for GOME (FRESCO)

The principle of the retrieval is explained by Fig. 1, which shows normalised spectra of the oxygen A-band for a clear and a cloudy pixel over the Atlantic Ocean. The data were acquired on 4 September 1998. In Fig. 1, the reflectivity in the continuum at 758 nm is 0.84 for the cloudy pixel, and 0.053 for the clear pixel. The cloud fraction is essentially derived from reflectivity in continuum, whereas cloud top pressure is derived from the depth of the absorption band.

In our retrieval method, called FRESCO (Fast Retrieval Scheme for Cloud Observables), three wavelength regions are used, around 758, 761, and 765 nm. It has been shown that the reflectivities at these three wavelength regions contain nearly all independent information which is available in the oxygen A-band (Kollewe et al, 1992). To simulate the spectrum of a (partly) cloudy GOME pixel, some assumptions are made in FRESCO. A pixel is assumed to consist of a clear and a cloudy part, of size $(1-c)$ and c, respectively, where c is the cloud fraction. To simplify the retrieval, all scattering processes are neglected. Only absorption above the cloud and surface due to oxygen is taken into account, as well as reflection by the surface or cloud top. The reflection by the surface and cloud is assumed to be Lambertian. Thus two paths through the atmosphere are possible in the model: (1) from the sun to the surface and back to the satellite, and (2) from the sun to the cloud top and back
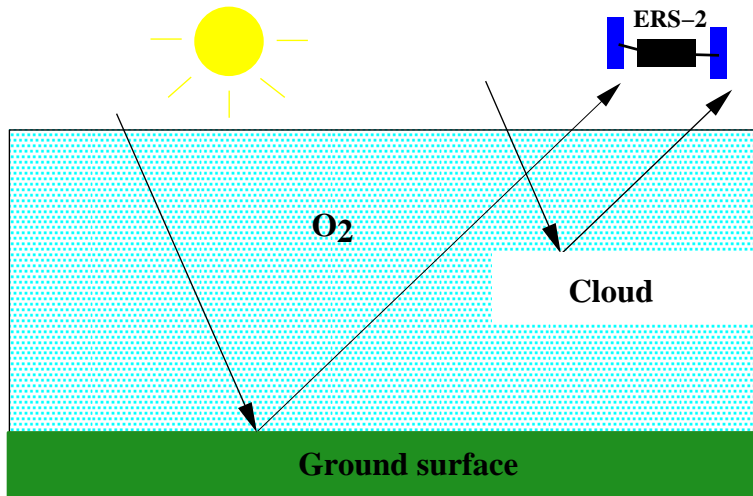
2

Figure 2: The two ray-paths of the reflection and absorption model used by FRESCO to simulate the spectrum of a partly cloudy pixel.

to the satellite. Along these paths, shown in Fig. 2, attenuation of the directly transmitted beam occurs due to absorption by oxygen. With these approximations, the simulated reflectivity R_{sim} can be written as

$$R_{sim} = (1 - c) \, T(\lambda, p_s, \mu, \mu_0) \, A_s + c \, T(\lambda, p_c, \mu, \mu_0) \, A_c, \tag{1}$$

where c is the cloud fraction, $T(\lambda, p, \mu, \mu_0)$ is the atmospheric transmittance for directly transmitted radiation, A_s and A_c are the surface and cloud top albedo, and p_s and p_c are the surface and cloud top pressures, respectively. The transmittance is multiplied by a geometrical correction factor to account for the Earth's sphericity at low solar elevations.

Cloud fraction and cloud top pressure are derived by non-linear least-squares minimisation of the difference between the measured and the simulated spectrum. For this minimisation, the Levenberg-Marquardt method is used. Since the atmospheric transmittance depends strongly on wavelength, line-by-line transmittances were calculated using HITRAN '96 data (Gamache et al., 1998). Afterwards, these high resolution transmittances were convoluted with the GOME slit function. For the calculations, a Mid-Latitude Summer atmosphere (Anderson et al., 1986) is assumed. Surface pressure over sea is taken to be 1013 hPa; over land a correction for surface elevation is applied. The surface elevation is deduced from the ETOPO-5 database. The surface albedo over ocean is taken to be 0.02, and over land it is deduced from minimum-reflectivity database composed from GOME data itself. A cloud albedo of 0.8 assumed, a choice which is optimised for ozone column retrieval (Koelemeijer and Stammes, 1999b). However, over surfaces with low surface albedo, such as over sea, it can easily be shown analytically that the FRESCO cloud top pressure are insensitive to the assumed value for the cloud albedo. Clearly, due to the assumption A_c=0.8, the cloud fraction should be interpreted as an *effective* cloud fraction for clouds with an albedo of 0.8.

3 Sensitivity analysis for FRESCO

To investigate the sensitivity of the FRESCO cloud fractions and cloud top pressures to measurement errors and retrieval assumptions, a sensitivity study has been performed. Six experiments were carried out, which are listed below. The differences in the retrieved cloud fraction Δc and cloud top pressure Δp_c are listed in Table 1.

1. Variation of wavelength λ with 0.04 nm, which is comparable to the accuracy of the wavelength calibration of GOME in this spectral region.

2. Relative error in the GOME reflectivity of 5% for all wavelengths. The accuracy of the GOME reflectivities (at least in the continuum) is of the order of 2-3%.

3. Relative error in the GOME reflectivity of 2% at non-absorbing or moderately absorbing wavelengths, and 5% for strongly absorbing wavelengths.

4. Replacement of the Mid-Latitude Summer profile by the Tropical profile.

5. Variation of the assumed surface albedo by ± 0.05.

6. Change in cloud albedo to 0.6 instead of 0.8.

Table 1: Results of sensitivity analysis FRESCO

Experiment	Δc	Δp_c
1) $\lambda \pm 0.04$ nm	< 0.005	< 20 hPa
2) $R_{meas} \pm 5\%$ ($\forall \lambda$)	< 0.05	< 40 hPa
3) $R_{meas} \pm 5\%$ (λ=761 nm)		
$R_{meas} \pm 2\%$ (λ=758, 765 nm)	< 0.02	< 15 hPa
4) MLS profile $\to$ TRO profile	< 0.005	< 5 hPa
5) $A_s \pm 0.05$	see below	< 30 hPa ($c > 0.5$)
		$\sim$ 150 hPa ($c < 0.2$)
6) $A_c = 0.8 \to A_c = 0.6$	see below	< 40 hPa (over land)
		< 5 hPa (over sea)

For experiments 1-4, the difference in the retrieved cloud fraction is < 0.05, and the difference in the retrieved cloud top pressure is < 40 hPa, which is sufficient for our application. We note that the assumed temperature profile has a neglegible influence on the derived cloud fraction and cloud top pressure, as follows from experiment 4. In experiments 5 and 6, the change in the retrieved cloud fraction agrees with that expected from theoretical considerations: in practice, c is determined by the reflectivity in continuum. Thus, c depends on the assumed cloud albedo A_c and surface albedo A_s according to

$$c = \frac{R_{sim} - A_s}{A_c - A_s}, \tag{2}$$

which is obtained from Eq. 1 by setting T=1, which is true for the continuum. In experiment 5, the change in cloud top pressure depends strongly on cloud fraction; for small cloud fractions, large errors in cloud top pressure may result from errors in the assumed surface albedo.

4   Cloud retrieval method for ATSR-2

Collocated measurements of the Along Track Scanning Radiometer-2 (ATSR-2) (Mutlow et al., 1994) have been analysed to yield an effective cloud fraction and cloud top pressure. Fourteen ATSR-2 images were analysed, acquired over North-West Europe on 23 July 1995, which are parts of ERS-2 orbits 1336 and 1337. To derive cloud fraction, we developed a cloud detection algorithm to separate cloud-free and cloudy pixels in a ATSR-2 images. This algorithm employs four tests to detect if a pixel is cloudy or clear. In the cloud detection algorithm, reflectivity measurements made at 0.66μm and 0.87μm are used, denoted by $R_{0.66}$ and $R_{0.87}$, as well as brightness temperature measurements made at 11μm and 12μm, denoted by T_{11} and T_{12}. If one of the tests determines the pixel as cloudy, it is designated as a cloudy pixel; only if all tests indicate that a pixel is cloud-free , it is designated as a clear pixel. The first test makes use of the fact that clouds are generally brighter than the surface. Therefore, if $R_{0.66}$ exceeds a specified threshold, the pixel is designated as cloudy. The second test
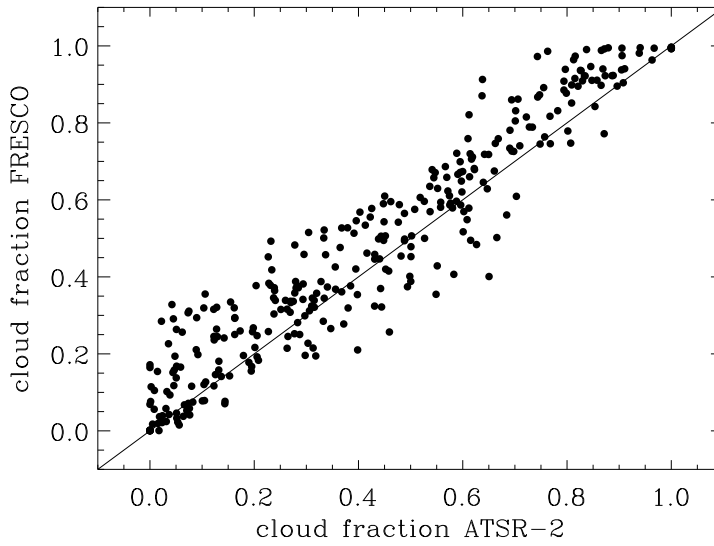
Figure 3: Correlation between FRESCO and ATSR-2 cloud fractions. The data were acquired on 23 July 1995, over North-West Europe.

makes use of the fact that clouds are generally colder than the surface. Therefore, if T_{11} is lower than a certain threshold, the pixel is designated as cloudy. The third test considers the spectral behaviour of the pixel. Since clouds are generally more spectrally white than the surface, a pixel is designated as cloudy if the ratio $R_{0.87}/R_{0.66}$ is close to unity. The fourth test is used to detect semi-transparent clouds, by considering the brightness temperature difference T_{11}-T_{12}, which is large for semi-transparent clouds, but small for clear sky conditions and for optically thick clouds. The thresholds are determined from histogram analysis.

After cloud detection, an effective cloud fraction c is derived for all cloudy pixels according to (cf. Eq. 2)

$$c = \frac{R_{0.66} - R_{clear}}{R_{cloud} - R_{clear}}, \tag{3}$$

where R_{clear} is the reflectivity of a clear case (obtained from cloud-free pixels), and R_{cloud}=0.8, similar to FRESCO. The effective cloud fractions of all ATSR-2 pixels within a GOME ground pixel have been averaged linearly to obtain the average effective cloud fraction.

To derive cloud top pressure, 11μm brightness temperature measurements were converted to pressures using pressure-temperature profiles from the European Center for Medium-range Weather Forecast (ECMWF) model. Only cloudy ATSR-2 pixels were selected with a brightness temperature difference between the 11μm and 12μm channels of $\leq$ 1K, to ensure that the cloud emissivity is close to unity, and that the measured brightness temperature is representative for the cloud top temperature. For the present analysis, no attempt was made to correct the cloud top temperatures for the effect of water vapour absorption. Maximally, there can be about 3200 ATSR-2 pixels in a GOME pixel. Only an average ATSR-2 cloud top pressure is derived for a GOME pixel if the number of ATSR-2 pixels in a GOME pixel with 11μm and 12μm $\leq$ 1K is larger than 500.

5   FRESCO results compared to ATSR-2 results

The relation FRESCO and ATSR-2 derived effective cloud fractions is shown in Fig. 3, and the relation between the derived cloud top pressures in Fig. 4. Table 5 lists the average difference, the RMS difference and the linear correlation coefficient of the FRESCO and ATSR-2 cloud fractions and cloud
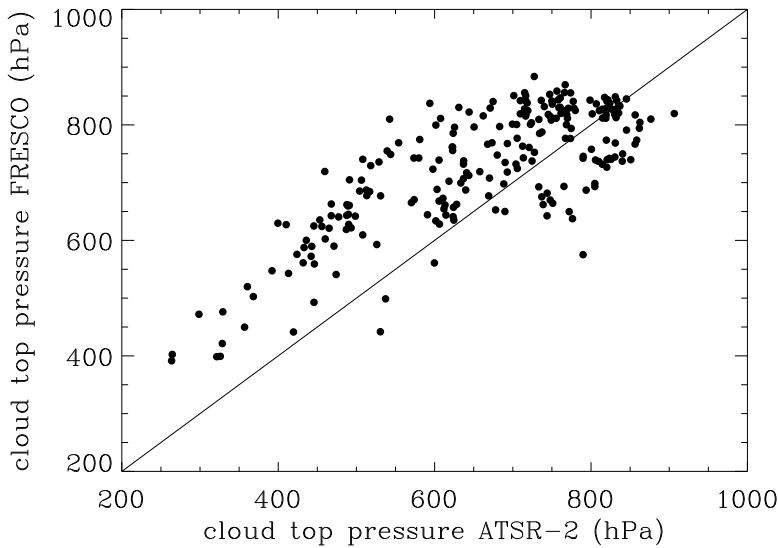
Figure 4: similar to Fig. 3, but for cloud top pressure.

top pressures. For the effective cloud fraction, a good correlation is found, although FRESCO cloud fractions are slightly higher than those of ATSR-2. The overestimation of c by FRESCO for small cloud fractions could be due to underestimation of the surface albedo by FRESCO. The overestimation of c by FRESCO for high cloud fractions could be due to the fact that FRESCO retrieves cloud fractions from the spatially average reflectivity, whereas the cloud fractions from ATSR-2 are derived for each individual ATSR-2 pixel, and are averaged over the GOME pixel afterwards. Although ATSR-2 pixels may have a reflectivity exceeding 0.8, the cloud fraction of these pixels never exceeds unity. Therefore, when averaging the cloud fractions of ATSR-2 over a GOME pixel, we may expect a systematic overestimation of the FRESCO cloud fraction compared to ATSR-2 for cases where the effective cloud fraction approaches unity.

The correlation between FRESCO and ATSR-2 cloud top pressures is weaker than for the cloud fractions, and shows more scatter. To investigate the reasons for differences between ATSR-2 and FRESCO cloud top pressures, a number of possible causes were considered, the conclusions of which are summarized here. First, it appears that the scatter between ATSR-2 and FRESCO decreases as the number of used ATSR-2 pixels within a GOME pixel increases, and may thus explain the random difference to some extent. No correlation was found between the cloud top pressure differences and the spatial variability within the GOME pixel, as was concluded by considering the spatial standard deviations of T_{11} and $R_{0.66}$ within a GOME pixel. However, a correlation was found between the difference between FRESCO and ATSR-2 cloud top pressures and the average cloud top reflectivity of the cloudy pixels as derived from the ATSR-2 measurements at 0.66μm. This is shown in Fig. 5. Apparently, if clouds have a high reflectivity (optically thick clouds), then the difference is large, whereas for optically thinner clouds, the difference is small. This may indicate that neglecting multiple scattering and absorption in clouds, which is a more severe approximation for optically thick clouds, explains part of the difference between FRESCO and ATSR-2 cloud top pressures.

Table 2: Statistics of comparison between FRESCO and ATSR-2 results

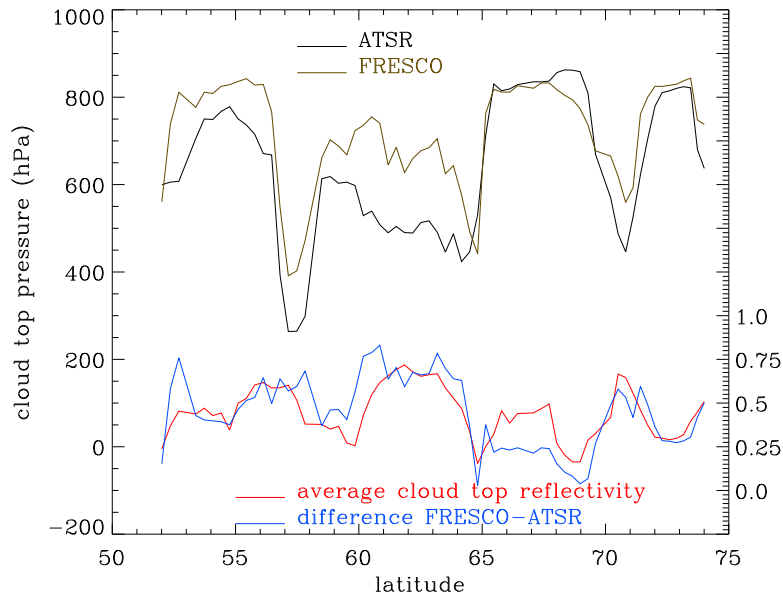| cloud parameter	average diff.	RMS diff.	linear corr. coeff.
cloud fraction	0.05	0.10	0.95
cloud top pressure	65 hPa	112 hPa	0.78

6

Figure 5: Cloud top pressures of FRESCO and ATSR-2, as well as their difference, in hPa. In addition, the average cloud top reflectivity is shown. The data are from ERS-2 orbit 1337.

6 Conclusions

We have shown that the principle to use the oxygen A-band method to derive cloud top pressure and cloud fraction works well. The advantage of using the oxygen A-band method as compared to the brightness temperature method, is that the first method is directly sensitive to pressure, as it was shown that the pressures derived with the oxygen A-band method are insensitive to the assumed temperature profile. A reasonable correlation was found between FRESCO cloud fractions and cloud top pressures and the same quantities derived from ATSR-2 data. The average difference between FRESCO and ATSR-2 cloud fractions is 0.05, the RMS difference is 0.10. The average difference in cloud top pressure is 65 hPa, the RMS difference is 112 hPa. We note that the FRESCO and ATSR-2 algorithms to derive cloud top pressure are completely different, as FRESCO employs the oxygen A-band, which is in the shortwave part of the Earth's spectrum, whereas the thermal infrared part of the Earth's spectrum is used to derive cloud top pressures from ATSR-2. Probably, part of the difference in the retrieved cloud top pressures is related to the neglection of multiple scattering and absorption within the cloud in FRESCO. Therefore, FRESCO cloud top pressures could be improved by making a correction for multiple scattering and absorption within the cloud. The FRESCO cloud fractions and cloud top pressures will be used for (near-real-time) ozone column retrieval at KNMI, in the framework of the GOME Ozone Fast Delivery and Value-Added Products (GOFAP) project (Piters et al., 1999).

Acknowledgements

References

1. Anderson, G. P., S. A. Clough, F. X. Kneizys, J. H. Chetwynd, and E. P. Shettle, AFGL atmospheric constituent profiles, *Tech. Rep. AFGL-TR-86-0110,* Air Force Geophys. Lab., Hanscom AFB, Mass.,

1986.

2. Burrows, J. P., et al., The Global Ozone Monitoring Experiment (GOME): Mission concept and first scientific results, *J. Geophys. Res., 56,* 151-175, 1999.

3. Chapman, R. M., Cloud distributions and altitude profiles from a satellite, *Planet. Space Sci., 9,* 71-71, 1962.

4. Deutsches Zentrum für Luft- und Raumfahrt (DLR), GOME level 1 to 2 algorithms description, *Tech. Rep. ER-TN-DLR-GO-0025,* 32 pp., DLR, Oberpfaffenhofen, Germany, 1994.

5. Fischer, J. and H. Grassl, Detection of cloud-top height from backscattered radiances within the oxygen A band. Part 1: Theoretical study, *J. Appl. Meteor., 30,* 1245-1259, 1991.

6. Gamache, R. R., A. Goldman, and L. S. Rothman, Improved spectral parameters for the three most abundant isotopomers of the oxygen molecule, *J. Quant. Spectrosc. Radiat. Transfer, 59,* 495-509, 1998.

7. Koelemeijer, R. B. A. and P. Stammes, Validation of Global Ozone Monitoring Experiment cloud fractions relevant for accurate ozone column retrieval, *J. Geophys. Res.,* 1999a, in press.

8. Koelemeijer, R. B. A. and P. Stammes, Effects of clouds on ozone column retrieval from GOME UV measurements, *J. Geophys. Res., 104,* 8281-8294, 1999b.

9. Kollewe, M., W. Cordes, and J. Fischer, Measurement and interpretation of the sunlight backscattered from clouds within the oxygen-A absorption band, in: Proceedings of the Central Symposium of the International Space Year, Munich, Germany, 30 March - 4 April 1992, ESA SP-341, ESA-ESTEC, Noordwijk, pp. 311-315, 1992.

10. Kuze, A., and K. V. Chance, Analysis of cloud top height and cloud coverage from satellites using the O_2 A and B bands, *J. Geophys. Res., 99,* 14,481-14,491, 1994.

11. Mutlow, C. T., A. M. Zàvody, I. J. Barton, and D. T. Llewellyn-Jones, Sea surface temperature measurements by the along-track scanning radiometer on the ERS-1 satellite: Early results, *J. Geophys. Res., 99,* 22,575-22,588, 1994.

12. O'Brien, D. M. and R. M. Mitchell, Error estimates for retrieval of cloud-top pressure using absorption in the A band of oxygen, *J. Appl. Meteor., 31,* 1179-1192, 1992.

13. Piters, A. J. M., P. J. M. Valks, and D. M. Stam, GOME ozone fast delivery and value-added products algorithm specification document, *Tech. Rep. GOFAP-KNMI-ASD-01,* 23 pp., KNMI, De Bilt, The Netherlands, 1999.

14. Rossow, W. B. and L. C. Garder, Cloud detection using satellite measurements of infrared and visible radiances for ISCCP, *J. Climate, 6,* 2341-2369, 1993.

15. Saiedy, F., H. Jacobowitz, and D. Q. Wark, On cloud-top determination from Gemini-5, *J. Atmos. Sci., 24,* 63-69, 1967.

16. Vanbauce, C., J. C. Buriez, F. Parol, B. Bonnel, G. Sèze, and P. Couvert, Apparent pressure derived from ADEOS-POLDER observations in the oxygen A-band over ocean, *Geophys. Res. Lett., 25,* 3159-3162, 1998.

17. Wu, M.-L. C., Remote sensing of cloud-top pressure using reflected solar radiation in the oxygen A-band, *J. Climate and Appl. Meteor., 24,* 593-546, 1985.

18. Yamamoto, G. and D. Q. Wark, Discussion of the letter by R. A. Hanel, 'Determination of Cloud Altitude from a Satellite,' *J. Geophys. Res., 66,* 3596, 1962.